

UCLA

UCLA Previously Published Works

Title

Multi-delay arterial spin labeling perfusion MRI in moyamoya disease-comparison with CT perfusion imaging

Permalink

<https://escholarship.org/uc/item/2wg6s658>

Journal

European Radiology, 24(5)

ISSN

0938-7994

Authors

Wang, Rui
Yu, Songlin
Alger, Jeffry R
[et al.](#)

Publication Date

2014-05-01

DOI

10.1007/s00330-014-3098-9

Peer reviewed

Multi-delay arterial spin labeling perfusion MRI in moyamoya disease—comparison with CT perfusion imaging

Rui Wang · Songlin Yu · Jeffrey R. Alger · Zhentao Zuo ·
Juan Chen · Rong Wang · Jing An · Bo Wang ·
Jizong Zhao · Rong Xue · Danny J. J. Wang

Received: 16 September 2013 / Revised: 27 November 2013 / Accepted: 14 January 2014 / Published online: 21 February 2014
© European Society of Radiology 2014

Abstract

Objectives To present a multi-delay pseudo-continuous ASL (pCASL) protocol that offers simultaneous measurements of cerebral blood flow (CBF) and arterial transit time (ATT), and to study correlations between multi-delay pCASL and CT perfusion in moyamoya disease.

Electronic supplementary material The online version of this article (doi:10.1007/s00330-014-3098-9) contains supplementary material, which is available to authorized users.

R. Wang · Z. Zuo · B. Wang · R. Xue (✉)
State Key Laboratory of Brain and Cognitive Science, Beijing MRI Center for Brain Research, Institute of Biophysics, Chinese Academy of Sciences, 15 Datun Road, Chaoyang District, Beijing 100101, China
e-mail: rxue@bcslab.ibp.ac.cn

R. Wang
Graduate School, University of Chinese Academy of Sciences, Beijing 100049, China

S. Yu · R. Wang · J. Zhao
Department of Neurosurgery, Beijing Tiantan Hospital, Capital Medical University, Beijing 100050, China

S. Yu · J. R. Alger · D. J. J. Wang
Department of Neurology, University of California Los Angeles, Los Angeles 90095, USA

R. Wang · J. R. Alger · R. Xue · D. J. J. Wang
UCLA-Beijing Joint Center for Advanced Brain Imaging, Beijing, China

R. Wang · J. R. Alger · R. Xue · D. J. J. Wang
UCLA-Beijing Joint Center for Advanced Brain Imaging, Los Angeles, CA, USA

J. Chen
Department of Radiology, Beijing Hospital, Beijing 100730, China

J. An
Siemens Shenzhen Magnetic Resonance Ltd, Shenzhen 518057, China

Methods A 4 post-labeling delay (PLD) pCASL protocol was applied on 17 patients with moyamoya disease who also underwent CT perfusion imaging. ATT was estimated using the multi-delay protocol and included in the calculation of CBF. ASL and CT perfusion images were rated for lesion severity/conspicuity. Pearson correlation coefficients were calculated across voxels between the two modalities in grey and white matter of each subject respectively and between normalized mean values of ASL and CT perfusion measures in major vascular territories.

Results Significant associations between ASL and CT perfusion were detected using subjective ratings, voxel-wise analysis in grey and white matter and region of interest (ROI)-based analysis of normalized mean perfusion. The correlation between ASL CBF and CT perfusion was improved using the multi-delay pCASL protocol compared to CBF acquired at a single PLD of 2 s ($P < 0.05$).

Conclusions There is a correlation between perfusion data from ASL and CT perfusion imaging in patients with moyamoya disease. Multi-delay ASL can improve CBF quantification, which could be a prognostic imaging biomarker in patients with moyamoya disease.

Key Points

- Simultaneous measurements of CBF and ATT can be achieved using multi-delay pCASL.
- Multi-delay ASL was compared with CT perfusion in patients with moyamoya disease.
- Statistical analyses showed significant associations between multi-delay ASL and CT perfusion.
- Multi-delay ASL can improve CBF quantification in moyamoya disease.

Keywords Magnetic resonance imaging · Arterial spin labeling · Perfusion · Moyamoya disease · Multidetector computed tomography

Abbreviations

ACA	Anterior cerebral artery
ATT	Arterial transit time
bSVD	Block-circulant singular-value decomposition
CBF	Cerebral blood flow
CBF _{mean}	Mean of the estimated CBF at each PLD
CBF _{2,000}	CBF calculated using the typical PLD of 2,000 ms
CBV	Cerebral blood volume
CTP	CT perfusion
GRASE	Gradient and spin echo
MRI	Magnetic resonance imaging
MCA	Middle cerebral artery
pCASL	Pseudo-continuous arterial spin labeling
PLD	Post-labeling delay
ROI	Region of interest

Introduction

Arterial spin labeling (ASL) offers a non-invasive method for quantifying cerebral blood flow (CBF) by using magnetically labelled arterial blood water as an endogenous tracer. Owing to its completely non-invasive nature, perfusion measurement using ASL has been increasingly applied to imaging studies on neurologic and psychiatric diseases [1–3]. However, clinical evaluation studies have demonstrated the challenges of optimizing ASL acquisitions for subjects across a wide range of vascular and perfusion characteristics [4, 5]. The main limitation of ASL is that the time delay between labeling in the feeding arteries and the arrival of labelled blood in tissue (i.e. arterial transit time or ATT) can have a large effect on the ASL signal. In cerebrovascular disorders such as ischaemic stroke, steno-occlusive and moyamoya diseases, ATT is generally prolonged leading to focal intravascular signals, as well as underestimation of tissue perfusion—a phenomenon termed arterial transit effects.

Moyamoya disease is a cerebrovascular disease characterized by progressive stenosis or occlusion of terminal internal carotid arteries (ICAs), which leads to extensive collateral formation. However, these collaterals are imperfect, and patients are prone to acute ischaemic stroke or brain haemorrhage [1]. CT perfusion (CTP) imaging, although not considered to be the gold standard given known errors related to bolus-based perfusion measurement [6], is a common method that has been relatively widely used in clinical practice for brain perfusion measurement. CTP is routinely applied for evaluating cerebral hemodynamics in moyamoya disease because it provides relatively accurate perfusion quantification including CBF, cerebral blood volume (CBV) and mean transit time (MTT) [7]. The disadvantages of CTP include the radiation dose and that iodinated contrast material may be unsuitable for some patients [8]. While ASL would be ideal

for (repeated) assessments of hemodynamics in patients with moyamoya disease, the markedly prolonged arterial transit delays [9] resulting from extensive collaterals may affect the accuracy of perfusion quantification.

Limited by the relatively long scan time required, very few studies have attempted the multi-delay ASL approach in cerebrovascular disorders to simultaneously estimate ATT and CBF [5, 10]. This issue has recently been addressed by combining single-shot 3D GRASE (gradient and spin echo), background suppression and pseudo-continuous ASL (pCASL), which resulted in dramatic improvements in the temporal stability of ASL image series [11]. In this study, we present a multi-delay ASL protocol using 3D background-suppressed 3D GRASE pCASL to achieve simultaneous measurements of CBF and ATT in relatively short times in patients with moyamoya disease.

The goals of our research were to study correlations between multi-delay pCASL and CT perfusion in moyamoya disease, and to compare CBF values obtained using multi-delay pCASL and those calculated using a single post-labeling delay (PLD) of 2 s. We propose that multi-delay pCASL would provide a comparable non-invasive assessment of brain perfusion in moyamoya disease in comparison to the more widely used CT perfusion.

Materials and methods

Patients

This prospective study received institutional review board approval. Informed consent was obtained from all patients. Between July 2011 and February 2012, 17 patients (6 F/11 M, mean age 36.2±14.3 years) angiographically diagnosed as having Moyamoya disease and evaluated for surgical revascularization were enrolled in this study. The exclusion criteria included patients with intracranial haemorrhages or other brain lesions; patients with a history of contrast medium allergy or renal failure; serum glucose level less than 2.7 mmol/l or greater than 22.2 mmol/l; general contraindications for MR imaging examinations. Digital subtraction angiography (DSA) was reviewed to grade the severity of the disease according to Suzuki's classification [12]. This classification describes angiographic stages of progressive ICA occlusion and appearance of basal collateral vessels from stage 1 (bilateral terminal ICA stenosis) to stage 6 (complete obliteration of the ICA circulation with supply of brain derived entirely from the external carotid artery). The patients were categorized according to their clinical symptoms into the following classifications: moderate, patients with occasional (less than once a month) transient ischaemic attacks (TIAs) (category A, 9 patients); and severe, patients who had TIAs occurring more than once a month

or recurrent stroke within the previous 12 months (category B, 8 patients) (see table in Electronic Supplementary Material). Each subject was examined following an identical protocol. The time interval between preoperative CT perfusion and pCASL MRI was approximately 1–40 days (21.2 ± 12.9).

CT perfusion technique

CT perfusion was performed on a GE Discovery CT750 HD scanner and was initiated 10 s after injection of a bolus of 45 ml of iobitridol (300 mg/ml) at a rate of 5 ml/s into the antecubital vein (with a 20-gauge intravenous cannula) using a power injector. The acquisition parameters were as follows: 120 kVp, 250 mA, 0.5 s/rotation, 55-s CT data acquisition time. Four contiguous sections with a slice thickness of 5 mm and in-plane resolution of $0.98 \times 0.98 \text{ mm}^2$ from the level of the basal ganglia/internal capsules to the upper portion of the lateral ventricles were obtained (Fig. 2A, left). The effective dose of CTP was 40 mSv. Routine noncontrast CT was also acquired, which covered the entire brain with a spatial resolution of $0.49 \times 0.49 \times 5 \text{ mm}^3$ and was used for the purpose of coregistration.

MRI protocols

MRI was performed on a 3-T Siemens Trio Tim system using the body coil as a transmitter and 12-channel head coil as a receiver. The patients were examined using a pCASL pulse sequence with background-suppressed 3D GRASE readout [11]. Imaging parameters were as follows: labeling pulse duration, 1.5 s; 4 PLD, 1.5/2/2.5/3 s; no flow crushing gradient; rate-2 GRAPPA; TR, 3.5/3.9/4.4/4.9 s (TR varies with PLD); TE, 22 ms; voxel size, $3.44 \times 3.44 \times 5 \text{ mm}^3$; 26 slices covering the whole brain (Fig. 2A, right); 20 pairs of tag/control images were acquired for each delay with a total scan time of 11.2 min (4 PLDs). An M0 image was acquired using TR=6 s and PLD=4 s (scan time=12 s). In addition, a high resolution sagittal T1 MPRAGE image was acquired for coregistration and segmentation of the brain into grey and white matter as described below.

Data processing

Image analysis was performed using SPM8 (Wellcome Trust Centre for NeuroImaging, UCK, UK) and Matlab 2010a (MathWorks, Natick, MA). After motion correction, mean perfusion difference images, $\Delta M(i)$, were generated for each PLD (i). A weighted delay, WD, was calculated by Eq. (1) and converted into ATT or δ based on the theoretical relationship

between WD and ATT [13] (see Fig. 1 in the Electronic Supplementary Material).

$$\text{WD} = \left[\sum_{i=1}^4 w_i \Delta M(i) \right] / \left[\sum_{i=1}^4 \Delta M(i) \right] \quad (1)$$

CBF at each delay, $f(i)$, was calculated using the measured ATT map and the following equation [14]:

$$f(i) = \frac{\lambda \Delta M(i) R_{1a}}{2 \alpha M_0 [\exp((\min(\delta - w_i, 0) - \delta) R_{1a}) - \exp(-(\tau + w_i) R_{1a})]} \quad (2)$$

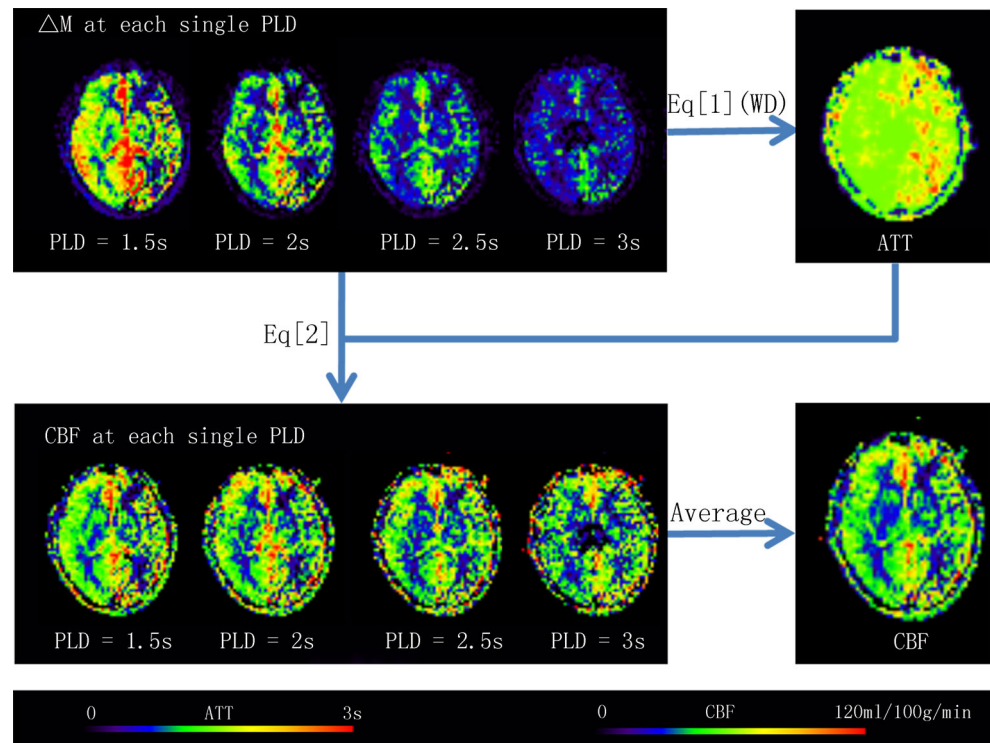
where R_{1a} ($= 0.61 \text{ s}^{-1}$) is the longitudinal relaxation rate of blood, M_0 is the equilibrium magnetization of brain tissue, α ($= 0.8$) is the tagging efficiency, τ ($= 1.5 \text{ s}$) is the duration of the labeling pulse, w_i ($= 1.5/2/2.5/3 \text{ s}$) is the post-labeling delay time, λ ($= 0.9 \text{ g/ml}$) is the blood/tissue water partition coefficient, and the final CBF was the mean of the estimated CBF at each PLD. The steps of the data processing are shown in Fig. 1.

The software used for CTP analysis was SCAN4 (developed in-house by JRA), which has been used in large-scale clinical trials [15]. Post-processing of CT perfusion images yielded multi-parametric perfusion maps including CBF, CBV and MTT by using the delay-insensitive block-circulant singular-value decomposition (bSVD) method according to previously described procedures [16]. For each voxel, the CBV map was calculated from the areas under the time–concentration curves. MTT was determined by the full width at half-maximum (FWHM) of the tissue residual function, and then CBF was calculated as CBV/MTT according to the central volume principle.

All ASL and CT perfusion images were registered to the T1-weighted MRI. The CT perfusion images were registered to T1-weighted MRI using the whole brain noncontrast CT as an interim template. MR images were then re-sliced into the space of CT perfusion images for all further analyses. T1-weighted images were segmented into grey matter (GM) and white matter (WM) probability maps, using the Segment program in SPM8. The GM and WM masks were generated by thresholding the corresponding probability maps at 90 %. Two neuroradiologists (with over 15 years of experience) blinded to clinical information independently and separately reviewed ASL and CT perfusion maps, which were scored on a scale of 0 to 3 to rate lesion severity/conspicuity [17].

ASL and CT perfusion images were further normalized into the Montreal Neurological Institute template space using SPM8. Subsequently, segmentation of ASL and CT perfusion images into major vascular territories was performed using an

Fig. 1 Diagram of the data processing steps to simultaneously obtain ATT and CBF images using the multi-delay pCASL protocol in a 25-year-old female patient with moyamoya disease with low perfusion in the left frontal and occipital lobes. CBF at each PLD is calculated using the measured ATT map and Eq. (2). The final CBF was the average of the estimated CBF at 4 PLDs



automated region-of-interest (ROI) analysis based on a published template of vascular territories in both hemispheres [18]. The vascular territories studied were anterior cerebral artery (ACA), leptomeningeal and lenticulostriate (perforator) distributions of the middle cerebral artery (MCA).

Statistical analysis

Statistical analysis was performed using the SPSS 16.0 software (SPSS, Chicago, IL). The following analyses were performed to assess the performance of ASL against CT perfusion: (1) Inter-rater reliability: the Kappa statistic was calculated to evaluate the reliability of ratings between the two readers; (2) voxel-wise analysis in grey and white matter: Pearson correlation coefficients were calculated across voxels between the two modalities in grey and white matter of each subject respectively; (3) ROI-based analysis of normalized mean perfusion: Pearson correlation coefficients were calculated between normalized mean values of ASL and CT perfusion measures in major vascular territories. Taking a CBF image as an example, the normalized mean value was defined as the mean CBF values of all voxels within an individual vascular territory ($\text{meanCBF}_{\text{ind}}$) divided by the mean of CBF values of the whole coverage (the same coverage with CTP) ($\text{meanCBF}_{\text{whole}}$), i.e. $\text{meanCBF}_{\text{ind}}/\text{meanCBF}_{\text{whole}}$. (4) In addition, comparison of the performance between $\text{CBF}_{2,000}$ (CBF calculated using the typical PLD of 2,000 ms) and CBF_{mean} (mean of the estimated CBF at each PLD) was

conducted. The Wilcoxon signed-rank test was applied to compare both voxel-wise and ROI-based correlation coefficients measured with $\text{CBF}_{2,000}$ vs. CTP CBF and CBF_{mean} vs. CTP CBF. The significance level was defined as $P < 0.05$ (2-sided).

Results

Ratings of hypoperfusion lesions

The clinical information of patients and calculated ATT distribution are provided in the table in the Electronic Supplementary Material. Table 1 lists the Kappa values (all $P < 0.01$) for lesion severity ratings of ASL and CTP between the two readers. Excellent inter-rater reliability ($\text{Kappa} > 0.75$) was achieved for CTP CBF hypoperfusion. Fair to good inter-rater reliability ($0.75 > \text{Kappa} > 0.55$) was achieved for ASL CBF hypoperfusion lesions as well as MTT and ATT prolongations. Overall, there was a good level of agreement between the two readers for each perfusion parameter. Spearman correlation coefficients between average conspicuity ratings of hypoperfusion lesions on multi-parametric ASL and CTP maps were also calculated. There were significant correlations between each pair of ASL and CT perfusion images: ASL ATT vs. CTP MTT ($r = 0.604$, $P = 0.01$) and ASL CBF vs. CTP CBF ($r = 0.512$, $P = 0.036$).

Table 1 Mean and SD of conspicuity ratings of 17 multi-parametric ASL and CTP perfusion images and Kappa of ratings between two readers

	ASL ATT Increase	ASL CBF Hypoperfusion	CTP MTT Increase	CTP CBF Hypoperfusion
Mean	1.50	1.56	1.41	1.26
SD	1.05	1.16	0.31	1.02
Kappa	0.606	0.589	0.675	0.759

Conspicuity rating criteria are score 3, the perfusion lesion can be identified definitely; score 2, relatively clear diagnosis of perfusion lesion can be drawn; score 1, possible diagnosis of perfusion lesion can be obtained; score 0, cannot afford any help to diagnosis

ASL arterial spin labeling, CTP CT perfusion, ATT arterial transit time, CBF cerebral blood flow, MTT mean transit time

Voxel-wise analysis in grey and white matter

Table 2 lists the mean and standard deviation of Pearson correlation coefficients between ASL and CTP across voxels in grey matter, white matter and whole coverage of each subject respectively. There were significant positive correlations (all $P < 0.001$) between the three pairs of parameters, i.e. ASL CBF_{mean} vs. CTP CBF, ASL CBF_{2,000} vs. CTP CBF and ASL ATT vs. CTP MTT, for each patient. The correlation coefficients between ASL CBF_{mean} and CTP CBF were increased compared to those between ASL CBF_{2,000} and CTP CBF in grey, white matter and whole coverage, suggesting improved accuracy of perfusion quantification using the multi-delay pCASL protocol ($P < 0.05$, Wilcoxon signed-rank test). Voxel-wise scatterplots and Pearson correlation coefficients of one representative case are shown in Fig. 3 in the Electronic Supplementary Material.

Figure 2B shows a representative case of moyamoya disease with coregistered ASL and CT perfusion images as well as the coverage of each imaging modality respectively (Fig. 2A). ASL has the advantage of (almost) whole brain coverage compared to CTP. By visual appearance, ASL

Table 2 Pearson correlation coefficient (mean ± SD, $n = 17$) between ASL and CTP

	Grey matter	White matter	Whole brain
ASL ATT vs. CTP MTT	0.47±0.065	0.702±0.041	0.712±0.063
ASL CBF _{mean} vs. CTP CBF	0.496±0.081*	0.495±0.058*	0.604±0.05*
ASL CBF _{2,000} vs. CTP CBF	0.46±0.103	0.469±0.074	0.576±0.088

ASL arterial spin labeling, CTP CT perfusion, ATT arterial transit time, CBF cerebral blood flow, MTT mean transit time, CBF_{mean} mean of the estimated CBF at each PLD, CBF_{2,000} CBF acquired at the single PLD of 2 s

*Significantly ($P < 0.05$) higher compared with ASL CBF_{2,000} vs. CTP CBF

perfusion maps showed similar perfusion lesions as CTP in the same slice, as well as hypoperfusion in superior slices that were not covered by CTP. Another representative patient with unilateral moyamoya disease is shown in Fig. 3 and multi-delay ASL images are in excellent concordance with the result of CTP.

ROI-based analysis of normalized mean perfusion

Figure 4 shows scatterplots and Pearson correlation coefficients between normalized mean values of ASL and CT perfusion parameters in the three major vascular territories. There were significant positive correlations between ASL ATT and CTP MTT in ACA, perforator MCA and leptomeningeal MCA ($r \geq 0.483$, $P < 0.05$). Significant associations between ASL CBF_{mean} and CTP CBF in perforator and leptomeningeal MCA territories ($r \geq 0.546$, $P < 0.05$) were observed. Again, the correlation coefficients between ASL CBF_{mean} and CTP CBF were increased compared to those between ASL CBF_{2,000} and CTP CBF in all three vascular territories, suggesting improved accuracy of perfusion quantification using the multi-delay pCASL protocol.

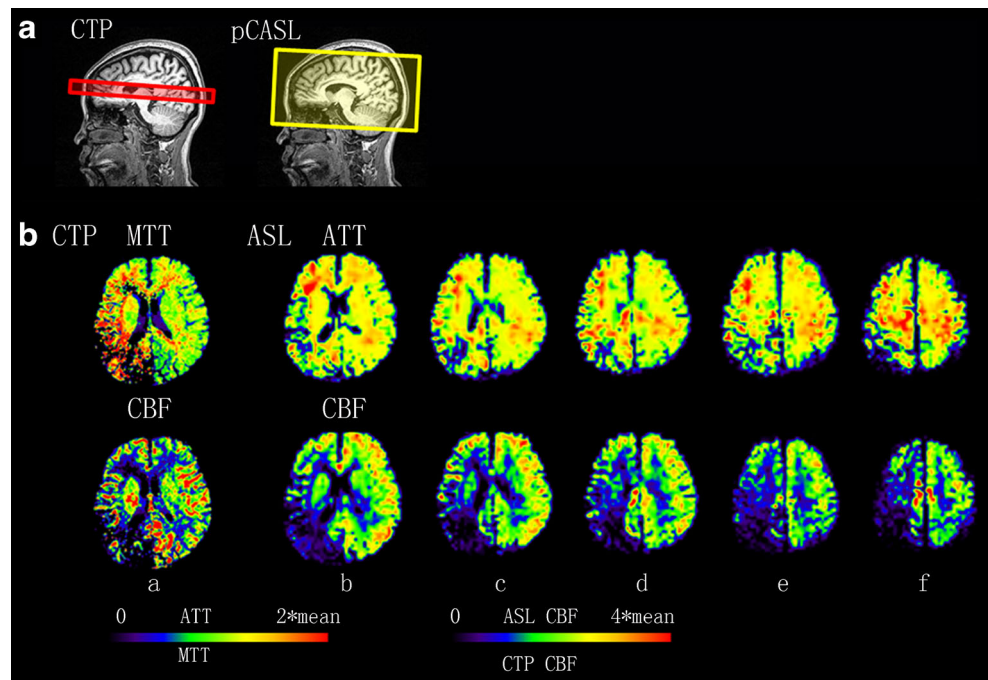
Evaluation of collateral flow through dynamic ASL image series

The multi-delay pCASL protocol also offered the capability for the evaluation of collateral flow through dynamic perfusion image series. Figure 5 shows serial pCASL CBF images at 4 PLDs (a), along with calculated multi-parametric pCASL (b) images of one representative case of moyamoya disease. The delayed arterial transit effects can be seen clearly in bilateral MCA territories (arrows) on multi-delay pCASL CBF images. The estimated ATT was prolonged in the affected region. By taking into account delayed ATT, CBF_{mean} generated using the multi-delay pCASL protocol was increased compared with CBF_{2,000} acquired at the single PLD of 2 s. Collateral flow was also accompanied by delayed arterial transit effects in multi-delay pCASL images. Figure 6 shows a representative case in which arterial transit effects (focal intravascular signals) were present (arrow) in the left parietal lobe with prolonged ATT. While pCASL perfusion images generally matched CTP images, arterial transit effects were unique to ASL.

Discussion

In this study, we presented a multi-delay pCASL protocol and performed correlation analyses between ASL and CT perfusion in a cohort of 17 patients with moyamoya disease. By incorporating delayed ATT into the CBF calculation, ASL was able to provide quantitative perfusion imaging consistent

Fig. 2 *A* Imaging coverage of CT perfusion and pCASL. *B* Perfusion maps generated from CTP (*a*) and ASL (*b–f*) in a 31-year-old male patient with episodes of dizziness and blurred vision for 6 months. CTP CBF (*a*) and ASL CBF (*b*) show hypoperfusion in the right frontal, occipital, temporal-parietal lobes. CTP MTT (*a*) and ASL ATT (*b*) were prolonged with hypoperfusion on CBF images. However, ATT is not or only slightly prolonged in the right posterior portion with extremely low CBF. Abnormal perfusion was also observed in ASL perfusion images in superior slices (*c–f*) that were not covered in CT perfusion



with CTP in moyamoya disease. The consistent associations between ASL CBF and CTP CBF, ASL ATT and CTP MTT

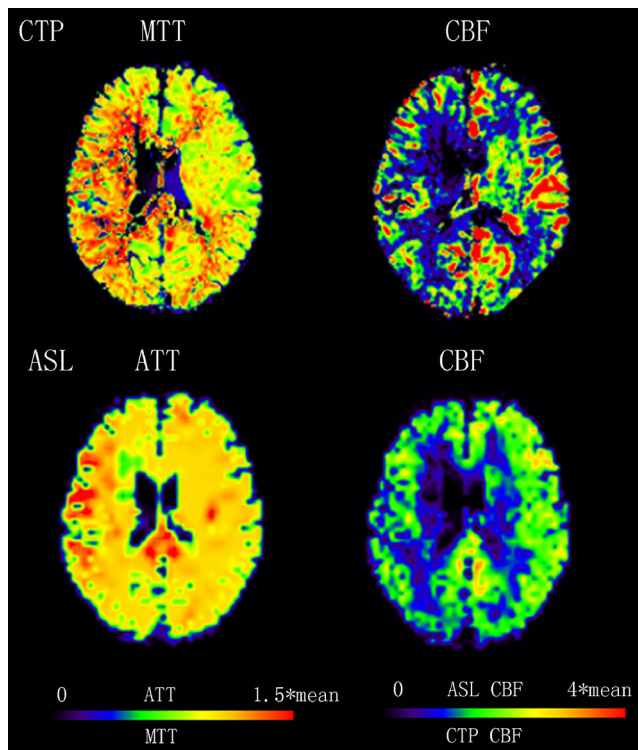


Fig. 3 Representative case of moyamoya disease with multi-parametric CTP and ASL images. A 24-year-old male patient with 6 months of transient headache and weakness in the left limb. The time interval between preoperative CT perfusion and pCASL was 1 day. CTP shows low perfusion areas in the right temporal-parietal lobe with decreased CBF values and elevated MTT. ASL is in concordance with the result of CTP

were demonstrated by subjective ratings as well as voxel-wise analysis in grey and white matter and ROI-based analysis of normalized mean perfusion. Previous studies conducted in healthy subjects have shown a good correlation between ASL CBF measurements and gold standard CBF imaging using ^{15}O -PET [19]. However, CBF may be underestimated in regions with delayed arterial arrival times, especially in cerebrovascular diseases [5]. Limited by the relatively long scan time required, very few studies have attempted the multi-delay ASL approach in cerebrovascular disorders to simultaneously estimate ATT and CBF [5, 10]. Most existing studies also employed nonlinear least-square fitting for analysing multi-delay ASL data, which may be unstable in the presence of low signal to noise ratio (SNR) and few sample points. In the present study, we combined pCASL and background-suppressed 3D GRASE to improve SNR and shorten image acquisition time, in conjunction with a robust algorithm for estimating ATT based on weighted delay [13]. The multi-delay pCASL protocol offers simultaneous estimation of CBF and ATT images within approximately 10 min and it could be shorter with fewer pairs of tag/control for each delay at the cost of SNR [10].

CBF is one of the most important parameters for determining the brain's condition. It is well known that the voluntary elevation of CBF suggests the active phase of the brain, and the pathological decrease of CBF can immediately cause a reversible or irreversible damaged state in brain tissues [20]. For moyamoya disease, a rare progressive intracranial vascular steno-occlusive disease of unknown aetiology, CBF obtained with ASL could be a prognostic imaging biomarker. Recent studies have generally used a single PLD, typically

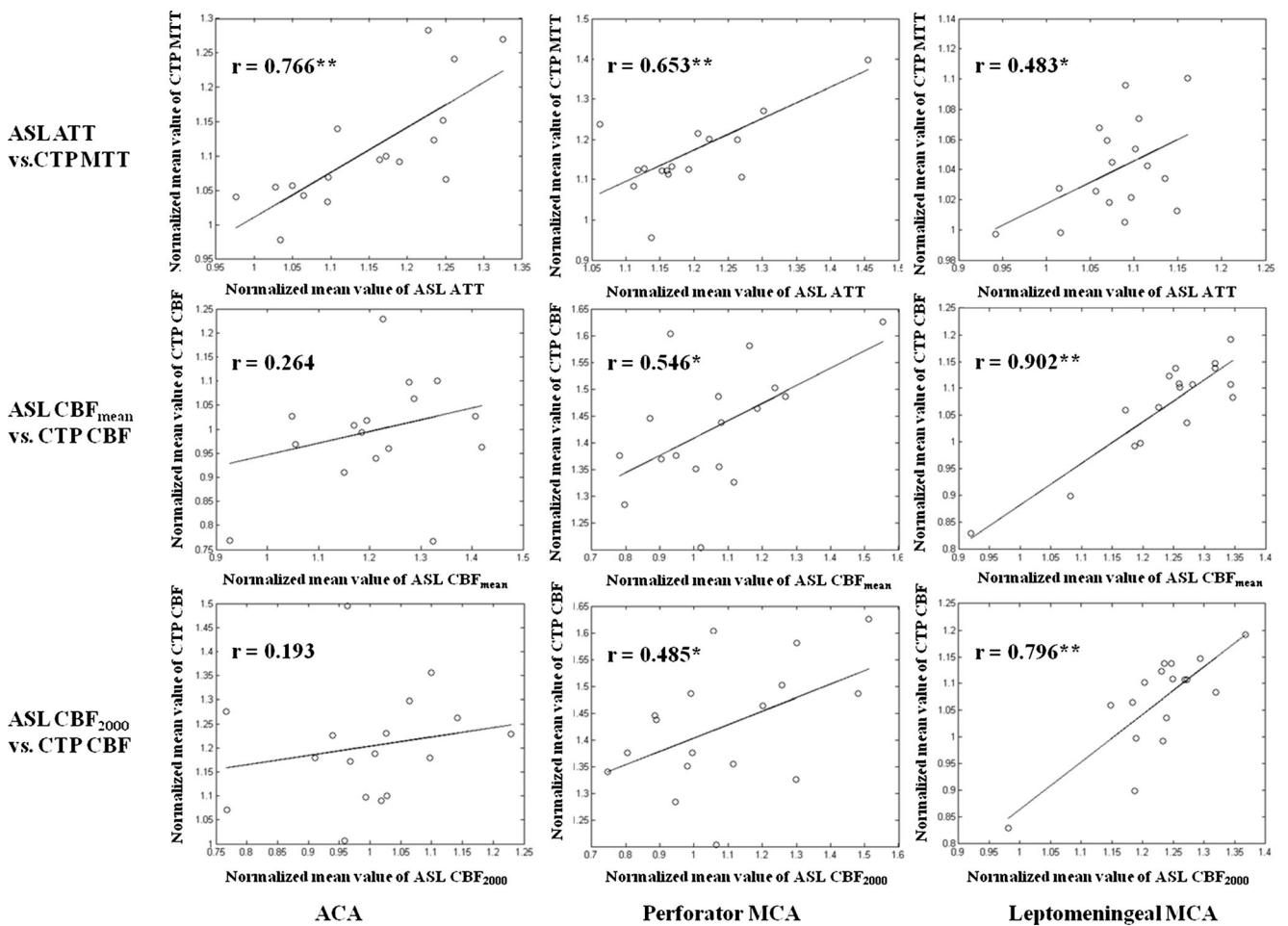
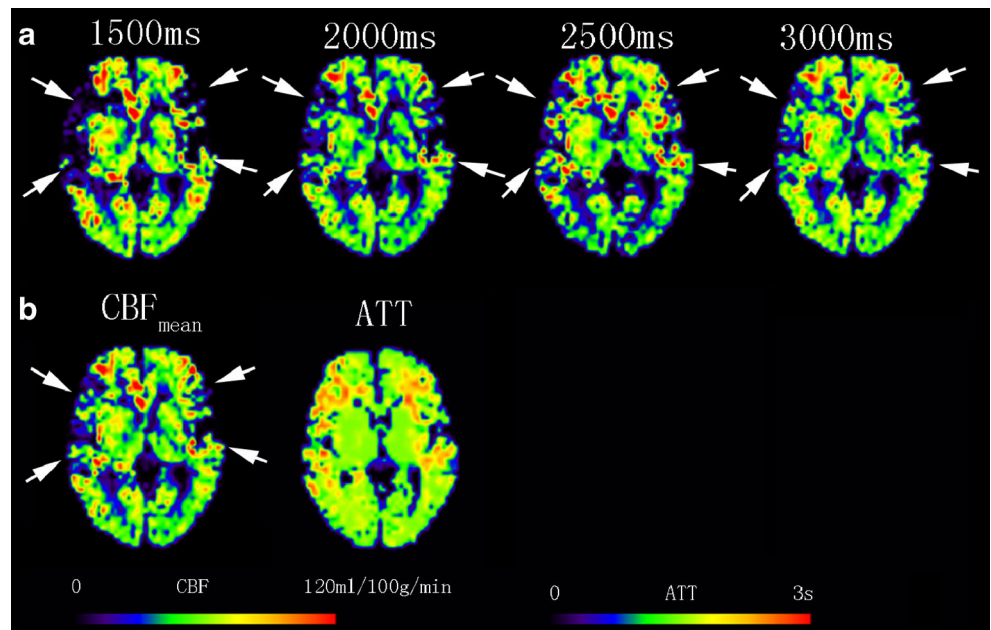


Fig. 4 Scatterplots and Pearson correlation coefficients between normalized average values of ASL and CTP in major vascular territories of all 17 scans (* $P < 0.05$; ** $P < 0.005$)

Fig. 5 a From left to right: pCASL CBF images for PLD of 1,500, 2,000, 2,500, 3,000 ms. **b** ASL CBF_{mean} and ATT images of the same slice in a 32-year-old female patient with moyamoya disease. PCASL with short PLD CBF maps showed enlarged abnormal perfusion territories (arrows) in bilateral frontal-temporal lobes with prolonged ATT, whereas the problem is mitigated in perfusion images with long PLDs and in CBF_{mean} image



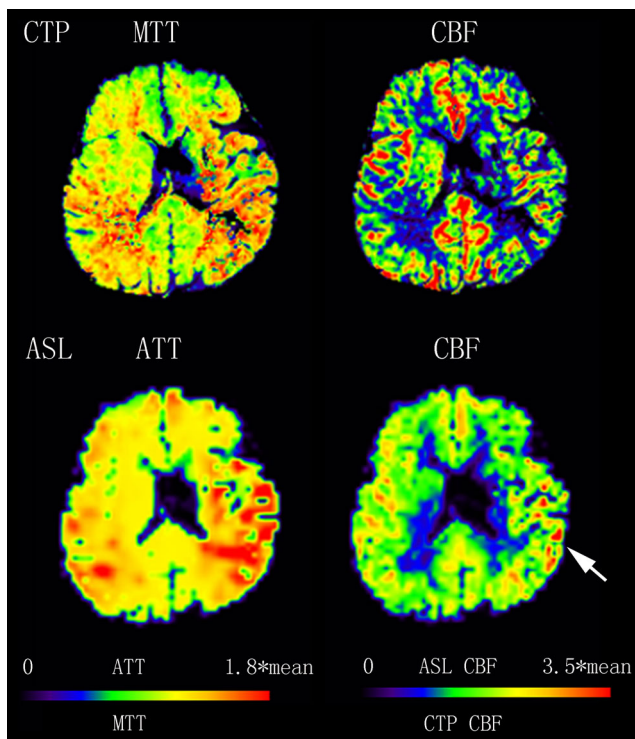


Fig. 6 A 48-year-old man with a history of paroxysmal weakness in the right limb for 15 years. CTP shows perfusion deficit in bilateral temporal-parietal lobes, posterior of basal ganglia and coronal radiate with decreased CBF values and elevated MTT. ASL perfusion images show almost the same perfusion changes as CTP. However, ASL CBF shows delayed transit effects in the left parietal lobe (*arrow*)

between 1.5 and 2 s in pCASL scans, as a trade-off between maintaining adequate diagnostic quality (SNR) and allowing sufficient delay for visualizing tissue perfusion at 1.5 T and 3 T [17, 21, 22]. Our finding indicated that ASL CBF_{mean} calculated using 4 PLDs was more accurate than ASL $CBF_{2,000}$ acquired at a single PLD of 2 s, using CTP as the reference standard. In particular, because the calculated CBF is the mean of the ATT adjusted CBF at 4 PLDs, there is minimal loss of SNR compared to single-delay pCASL scans with the same amount of scan time. The capability of the multi-delay pCASL protocol for non-invasive perfusion imaging within reasonable imaging time and without penalty in SNR makes it suitable in the clinical setting.

Another potential use of the multi-delay pCASL protocol is the evaluation of collateral flow through dynamic perfusion images. Recent clinical evaluation of ASL in cerebrovascular diseases suggested that delayed arterial transit effects characterized by focal intravascular signals and low tissue perfusion in ASL may indicate the status of collateral perfusion [3, 23, 24]. Zaharchuk et al. [21] reported that ASL can predict the presence and intensity of collateral flow in patients with moyamoya syndrome using DSA as the gold standard. A “borderzone” pattern has been identified using ASL in patients with suspected cerebrovascular diseases who had normal-appearing dynamic susceptibility contrast perfusion-

weighted imaging (DSC PWI) [25]. So far, the identification of delayed transit effects and the inference of collateral perfusion have been mainly based on “snap-shot” ASL images acquired at a single PLD, typically between 1.5 and 2 s. The proposed multi-delay pCASL approach is capable of providing visualization of collateral flow in moyamoya disease through dynamic perfusion image series, and the potential for quantitative assessment of collateral perfusion. In future clinical studies, it is recommended to examine dynamic perfusion image series at multiple PLDs in addition to the mean CBF and ATT maps.

For patients with moyamoya disease, it is necessary to evaluate brain perfusion for the consideration of bypass surgery preoperatively and for monitoring surgical effects postoperatively. Moyamoya disease is a chronic and progressive disease which makes regular brain perfusion examination necessary. Compared with CTP, ASL is totally free of radiation and exogenous contrast agent and thus can be applied in children and patients who have medical diseases such as renal insufficiency, hyperthyroidism or those who are allergic to iodinated contrast. It is more acceptable to both patients and radiologists owing to its safety and operability. The consistency between multi-delay ASL and CT perfusion images demonstrated in this study may render multi-delay ASL an alternative to CTP in patients with renal failure or diabetes mellitus. In this regard, multi-delay ASL may be combined with other MRI sequences, such as anatomic imaging, MR angiography and diffusion MRI to provide the most comprehensive information in one examination, leading to a high benefit/cost ratio without ionizing radiation or intravenous access.

This study has several limitations. Since a range of PLDs from 1.5 to 3 s in a step of 0.5 s were used, calculated ATT values less than 1.5 s or more than 3.0 s were truncated to 1.5 s and 3.0 s, respectively. As a result, we can only obtain the ATT maps within the range from 1.5 s to 3 s (measured ATT was largely within this range for the patients with moyamoya disease, see [table](#) in the Electronic Supplementary Material). The ATT value could not be calculated accurately when there was no signal in the ΔM image because of no flow ($CBF=0$) or very long transit times (full relaxation of the labelled blood, no signal in ASL image regardless of CBF). Meanwhile, we do not report absolute quantitative perfusion parameters using both ASL and CT perfusion. Although one of the advantages of CT perfusion imaging is its quantitative nature, it has been reported that the results of CT perfusion imaging analysis vary substantially owing to differences in scan parameters, post-processing steps and different algorithms [26]. It should also be kept in mind that CTP uses a non-diffusible tracer, whereas ASL uses a diffusible tracer. Therefore, the correlation of absolute perfusion values between ASL and CT perfusion could not be assessed. Furthermore, correlation with other important variables such as vascular status was not examined,

which may help determine the clinical impact of ASL in the management of patients with moyamoya disease. Further studies with larger samples will be performed to evaluate the prognostic value of ASL in moyamoya disease and confirm the results on 1.5-T magnets. Overall, the present study represents an initial step in exploring the clinical value of multi-delay ASL in the management of moyamoya through comparison with CT perfusion.

In summary, there is a correlation between perfusion data from ASL and CT perfusion in patients with moyamoya disease. By incorporating delayed ATT in the calculation of CBF, multi-delay ASL is able to improve CBF quantification that is consistent with CT perfusion in moyamoya disease. The capability of ASL to provide non-invasive perfusion information without the use of contrast agent offers the potential to include ASL as part of standard neuroimaging protocols in the management of moyamoya disease. Further study of other cerebrovascular diseases, including acute ischemic stroke, is warranted.

Acknowledgement The scientific guarantor of this publication is Rong Xue. The authors of this manuscript declare no relationships with any companies whose products or services may be related to the subject matter of the article. This study has received funding from the Ministry of Science and Technology (MOST) of China (grant number 2012CB825500, 2010IM030800), National Nature Science Foundation of China (NSFC) (grant number 30830101, 91132302, 90820307), CAS Knowledge Innovation Project (grant number KSCX2-YW-R-259), CAS Strategic Priority Research Program (grant number XDB02010001, XDB02050001) and US NIH grants (R01-MH080892, R01-NS081077 and R01-EB014922). No complex statistical methods were necessary for this paper. Institutional review board approval was obtained. Written informed consent was obtained from all subjects (patients) in this study. No study subjects or cohorts have been previously reported. Methodology: prospective, cross sectional study, multicenter study.

References

- Alsop DC, Detre JA, Grossman M (2000) Assessment of cerebral blood flow in Alzheimer's disease by spin-labeled magnetic resonance imaging. *Ann Neurol* 47:93–100
- Detre JA, Alsop DC, Vives LR, Maccotta L, Teener JW, Raps EC (1998) Noninvasive MRI evaluation of cerebral blood flow in cerebrovascular disease. *Neurology* 50:633–641
- Chalela JA, Alsop DC, Gonzalez-Atavales JB, Maldjian JA, Kasner SE, Detre JA (2000) Magnetic resonance perfusion imaging in acute ischemic stroke using continuous arterial spin labeling. *Stroke* 31:680–687
- Calamante F, Gadian DG, Connelly A (2002) Quantification of perfusion using bolus tracking magnetic resonance imaging in stroke: assumptions, limitations, and potential implications for clinical use. *Stroke* 33:1146–1151
- MacIntosh BJ, Lindsay AC, Kyliantiras I et al (2010) Multiple inflow pulsed arterial spin-labeling reveals delays in the arterial arrival time in minor stroke and transient ischemic attack. *AJNR* 31:1892–1894
- Wintermark M, Sesay M, Barbier E et al (2005) Comparative overview of brain perfusion imaging techniques. *Stroke* 36:e83–e99
- Kang KH, Kim HS, Kim SY (2008) Quantitative cerebrovascular reserve measured by acetazolamide-challenged dynamic CT perfusion in ischemic adult moyamoya disease: initial experience with angiographic correlation. *AJNR* 29:1487–1493
- Smith WS, Roberts HC, Chuang NA et al (2003) Safety and feasibility of a CT protocol for acute stroke: combined CT, CT angiography, and CT perfusion imaging in 53 consecutive patients. *AJNR* 24:688–690
- Calamante F, Ganesan V, Kirkham FJ et al (2001) MR perfusion imaging in moyamoya syndrome: potential implications for clinical evaluation of occlusive cerebrovascular disease. *Stroke* 32:2810–2816
- Wang DJJ, Alger JR, Qiao JX et al (2013) Multi-delay multi-parametric arterial spin-labeled perfusion MRI in acute ischemic stroke—comparison with dynamic susceptibility contrast enhanced perfusion imaging. *NeuroImage Clin* 3:1–7
- Fernandez-Seara MA, Edlow BL, Hoang A, Wang J, Feinberg DA, Detre JA (2008) Minimizing acquisition time of arterial spin labeling at 3 T. *Magn Reson Med* 59:1467–1471
- Suzuki J, Kodama N (1983) Moyamoya disease: a review. *Stroke* 14:104–109
- Dai W, Robson PM, Shankaranarayanan A, Alsop DC (2012) Reduced resolution transit delay prescan for quantitative continuous arterial spin labeling perfusion imaging. *Magn Reson Med* 67:1252–1265
- Wang J, Zhang Y, Wolf RL, Roc AC, Alsop DC, Detre JA (2005) Amplitude-modulated continuous arterial spin-labeling 3.0-T perfusion MR imaging with a single coil: feasibility study. *Radiology* 235:218–228
- Kidwell CS, Jahan R, Gombin J et al (2013) A trial of imaging selection and endovascular treatment for ischemic stroke. *N Engl J Med* 368(10):914–923
- Wintermark M, Maeder TJP, Schnyder P, Meuli R (2001) Quantitative assessment of regional cerebral blood flows by perfusion CT studies at low injection rates: a critical review of the underlying theoretical models. *Eur Radiol* 11:1220–1230
- Wang DJ, Alger JR, Qiao JX et al (2012) The value of arterial spin-labeled perfusion imaging in acute ischemic stroke: comparison with dynamic susceptibility contrast-enhanced MRI. *Stroke* 43:1018–1024
- Tatu L, Moulin T, Bogousslavsky J, Duvernoy H (1998) Arterial territories of the human brain: cerebral hemispheres. *Neurology* 50:1699–1708
- Ye FQ, Berman KF, Ellmore T et al (2000) H(2)(15)O PET validation of steady-state arterial spin tagging cerebral blood flow measurements in humans. *Magn Reson Med* 44:450–456
- Noguchi T, Kawashima M, Nishihara M, Hirai T, Matsushima T, Irie H (2013) Arterial spin-labeling MR imaging in moyamoya disease compared with clinical assessments and other MR imaging findings. *Eur J Radiol* 82:e840–e847
- Zaharchuk G, Do HM, Marks MP, Rosenberg J, Moseley ME, Steinberg GK (2011) Arterial spin-labeling MRI can identify the presence and intensity of collateral perfusion in patients with moyamoya disease. *Stroke* 42:2485–2491
- Qiu D, Straka M, Zun Z, Bammer R, Moseley ME, Zaharchuk G (2012) CBF measurements using multidelay pseudocontinuous and velocity-selective arterial spin labeling in patients with long arterial transit delays: comparison with xenon CT CBF. *J Magn Reson Imaging* 36:110–119
- Chen J, Licht DJ, Smith SE et al (2009) Arterial spin labeling perfusion MRI in pediatric arterial ischemic stroke: initial experiences. *J Magn Reson Imaging* 29(2):282–290
- Zaharchuk G (2011) Arterial spin label imaging of acute ischemic stroke and transient ischemic attack. *Neuroimaging Clin N Am* 21(2):285–301

25. Zaharchuk G, Bammer R, Straka M et al (2009) Arterial spin-label imaging in patients with normal bolus perfusion-weighted MR imaging findings: pilot identification of the borderzone sign. *Radiology* 252(3):797–807
26. Kudo K, Sasaki M, Yamada K et al (2010) Differences in CT perfusion maps generated by different commercial software: quantitative analysis by using identical source data of acute stroke patients. *Radiology* 254:200–209